

Iridium Cyclometalated Complexes with Axial Symmetry. Synthesis and Photophysical Properties of a *trans*-Biscyclometalated Complex Containing the Terdentate Ligand 2,6-Diphenylpyridine

Matthew Polson, Sandro Fracasso, Valerio Bertolasi, Marcella Ravaglia, and Franco Scandola*

Dipartimento di Chimica, Università di Ferrara, Via L. Borsari 46, 44100 Ferrara, Italy

Received October 14, 2003

The first example of an iridium biscyclometalated complex with a C₂N₂C 2,6-diphenylpyridine (dppy)-type ligand, [(4'-(4-bromophenyl)-2,2':6':2''-terpyridine)Ir(2,6-diphenyl-4-(4-tolyl)pyridine)](NO₃) (**1**), has been synthesized and characterized by various techniques such as X-ray crystallography, mass spectrometry, ¹H and ¹³C NMR, cyclic voltammetry, and both steady-state and time-resolved emission and absorption studies. Preliminary density functional theory calculations have also been conducted. **1** crystallizes in the monoclinic space group *P*₂₁/*n*. The crystallographic data are as follows: C₄₅H₃₁BrN₄IrO₃·2H₂O, *a* = 17.4308(4) Å, *b* = 9.0312(2) Å, *c* = 26.7601(7) Å, β = 104.496-(1)°, *V* = 4078.5(2) Å³, *Z* = 4. The relatively long Ir–C distances (2.122 and 2.094 Å) reflect the strong mutual *trans* effect of the cyclometalating carbons. The complex exhibits strong visible absorption and long-lived (1.7 μs) emission (λ_{max}, 690 nm) in room temperature solution. The inherent asymmetry of the coordination environment offers a unique directional character to the emitting excited state, which is predominately ligand-to-ligand charge transfer (dppy → 2,2':6':2''-terpyridine) in nature.

Introduction

Polypyridine complexes of divalent d⁶ metals have been widely studied, because of their useful spectroscopic and photophysical properties.¹ They are photostable and exhibit

strong absorptions in the visible region, usually associated with metal-to-ligand charge-transfer (MLCT) transitions. Their lowest excited states, which are triplet MLCT in character, are efficiently populated by ultrafast intersystem crossing processes brought about by the strong spin–orbit coupling of the metal ion. Their long excited-state lifetimes and high luminescent efficiencies are particularly useful for the study of photoinduced energy- or electron-transfer processes. Interest in this class of compounds has grown in relation to their possible use as molecular components for a variety of supramolecular systems and photochemical molecular devices.² Of particular interest are those mimicking functions of photosynthesis in nature, such as light-harvesting (artificial antenna systems) or charge separation (artificial reaction centers). For these reasons Ru(II) and Os(II) metal–polypyridine complexes of increasing complexity have been the main goal of the synthetic efforts of this field.³

In recent years, considerable interest has also been devoted to compounds of Ir(III). In contrast to those of the divalent metals, the polypyridine complexes of Ir(III) do not exhibit intense visible absorptions and are characterized by lowest lying ligand-centered (LC) π–π* states. More interesting are the complexes with C₂N cyclometalating ligands such

* Author to whom correspondence should be addressed. E-mail: snf@unife.it.

- (1) (a) Juris, A.; Balzani, V.; Barigelletti, F.; Campagna, S.; Belser, P.; Von Zelewsky, A. *Coord. Chem. Rev.* **1988**, *84*, 85. (b) Kalyanasundaram, K. *Photochemistry of Polypyridine and Porphyrin Complexes*, Academic: New York, 1992.
- (2) (a) Balzani, V.; Scandola, F. *Supramolecular Photochemistry*; Ellis Horwood: Chichester, U.K., 1991. (b) Balzani, V.; Credi, A.; Scandola, F. In *Transition Metals in Supramolecular Chemistry*; Fabbri, L., Poggi, A., Eds.; Kluwer: Dordrecht, The Netherlands, 1994; p 1. (c) Lehn, J.-M. *Supramolecular Chemistry—Concepts and Properties*; VCH: Weinheim, Germany, 1995. (d) Bignozzi, C. A.; Schoonover, J. R.; Scandola, F. *Prog. Inorg. Chem.* **1997**, *44*, 11.
- (3) (a) Scandola, F.; Chiorboli, C.; Indelli, M. T.; Rampi, M. A. In *Electron Transfer in Chemistry*; Balzani, V., Ed.; Wiley-VCH: Weinheim, Germany, 2001; Vol. III, Chapter 2.3, pp 337–408. (b) Campagna, S.; Serroni, S.; Puntoriero, F.; Di Pietro, C.; Ricevuto, V. In *Electron Transfer in Chemistry*; Balzani, V., Ed.; Wiley-VCH: Weinheim, Germany, 2001; Vol. V, Chapter 1.6, pp 186–214. (c) De Cola, L.; Belser, P. In *Electron Transfer in Chemistry*; Balzani, V., Ed.; Wiley-VCH: Weinheim, Germany, 2001; Vol. V, Chapter 1.3, pp 97–136.
- (4) (a) Sprouse, S.; King, K. A.; Spellane, P. J.; Watts, R. J. *J. Am. Chem. Soc.* **1984**, *106*, 6647. (b) Crosby, G. A. *J. Chim. Phys. Phys.-Chim. Biol.* **1967**, *64*, 160.
- (5) Tamayo, A. B.; Alleyne, B. D.; Djurovich, P. I.; Lamansky, S.; Tsyba, I.; Ho, N. N.; Bu, R.; Thompson, M. E. *J. Am. Chem. Soc.* **2003**, *125*, 7377.

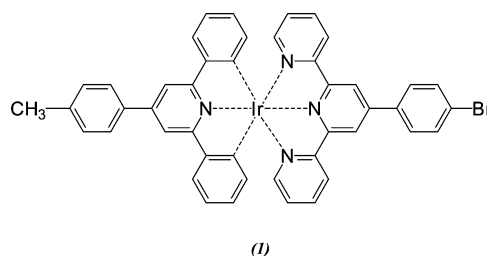
(6) Baldo, M. A.; Thompson, M. E.; Forrest, S. R. *Nature* **2000**, *403*, 750.

as, e.g., ppy (2-phenylpyridine). The metal–carbon bonds confer to these complexes properties which are distinct from those of N^N analogues: absorption in the visible region, lowest energy excited states of appreciable MLCT character well suited to participate in photoredox chemistry. The classic example is Ir(ppy)₃,⁴ which shows strong emission at 510 nm, with a high quantum yield ($\phi = 0.4$) and long excited-state lifetime (1.9 μ s) in fluid solution. The photophysical properties of cyclometalated complexes of Ir(III) make them very useful for several photonic applications.⁵ They have been of interest in the development of organic light-emitting devices (OLEDs). In this application, they can act either as triplet sensitizers of a fluorescent dye⁶ or as phosphorescent dyes,⁷ to overcome the efficiency limitations imposed by exciton spin statistics. These compounds can also be employed as sensitizers for outer-sphere electron-transfer reactions,⁸ photocatalysts for CO₂ reduction,⁹ photooxidants or singlet oxygen sensitizers,¹⁰ and labeling reagents for biological substrates.¹¹ They are also under investigation as possible candidates for the blue emitting unit of LED displays.¹²

If the metal complexes are to be used as building blocks for more complex supramolecular systems, not only their photophysical properties but also their structural type is important. From this viewpoint, complexes of terdentate ligands (such as, e.g., 2,2':6',2''-terpyridine, tpy) are definitely superior to those of bidentate ligands (e.g., 2,2'-bipyridine, bpy).¹³ Indeed, as opposed to most octahedral trisbidentate species, bisterdentate complexes are achiral (thus avoiding complications due to stereoisomers), and have axial symmetry (which permits connection to other molecular components without complications of geometrical isomerism). They are also convenient for synthetic reasons, due to the ease of substitution at the 4' position on the terpyridine ligand.^{13,14} Along with these structural advantages, however, tpy-type complexes may have drawbacks of photophysical nature. For example, Ru(II)–terpyridine complexes tend to have relatively short-lived MLCT states and to be weak emitters in solution, as a consequence of low excited-state

energy and/or efficient deactivation via upper metal-centered (MC) states.^{13,15} Until recently, little work has been done on terpyridine-based Ir(III) complexes, mainly because of the difficulty of their synthesis. A new methodology has been developed in the past few years which makes these complexes relatively accessible.¹⁶ These complexes exhibit high-energy absorption and emission. Their lowest excited states are of LC $\pi \sim \pi^*$ nature and decay on the microsecond time scale.

In this work we will describe a new Ir(III) complex which couples the good properties of terpyridine-type complexes (axial symmetry and substitutional ease) and of cyclometalated species (useful photophysics). Complex **1** involves two terdentate ligands: a N^N^N-bonded tpy derivative¹⁷ and a C^N^N-bonded dppy derivative (dppy = 2,6-diphenylpyridine). This heteroleptic arrangement gives the molecule a uniquely directional nature of its excited state. This is, to the best of our knowledge, the first biscyclometalated dppy complex of Ir(III).¹⁸



Experimental Section

Preparation of Compounds. [(4'-(4-Bromophenyl)-2:2',6':2''-terpyridine)IrCl₃] was synthesized according to the method of Collin et al.¹⁶ in 65% yield. 2,6-Diphenyl-4-(4-tolyl)pyridine was synthesized in a single step by the method of Cave et al.¹⁹ in 47% yield. The physical properties agreed with the literature values.

[(4'-(4-Bromophenyl)-2:2',6':2''-terpyridine)Ir(2,6-diphenyl-4-(4-tolyl)pyridine)](NO₃). A suspension of [(4'-(4-bromophenyl)-2:2',6':2''-terpyridine)IrCl₃] (100 mg, 0.14 mmol), 2,6-diphenyl-4-(4-tolyl)pyridine (70 mg, 0.15 mmol), and AgNO₃ (130 mg, excess) was heated to 190 °C in degassed ethylene glycol in the absence of direct light. On cooling, the suspension was filtered through Celite to remove AgCl and a black byproduct. The Celite plug was washed extensively with methanol. The organic solutions were combined and evaporated to remove the methanol. Water was added to precipitate the crude product, which was collected by filtration. The pure product was isolated by column chromatography on SiO₂ (prepared with an acetonitrile/saturated aqueous KNO₃ (10:1) solution), eluting with neat acetonitrile. The first eluted orange band

- (7) Lamansky, S.; Djurovich, P.; Murphy, D.; Abdel-Razzaq, F.; Lee, H.-E.; Adachi, C.; Burrows, P. E.; Forrest, S. R.; Thompson, M. E. *J. Am. Chem. Soc.* **2001**, *123*, 4304–4312.
- (8) (a) Sutin, N. *Acc. Chem. Res.* **1968**, *1*, 225. (b) Meyer, T. J. *Acc. Chem. Res.* **1978**, *11*, 94. (c) Schmid, B.; Garces, F. O.; Watts, R. J. *Inorg. Chem.* **1994**, *32*, 9.
- (9) (a) Belmore, K. A.; Vanderpool, R. A.; Tsai, J.-C.; Khan, M. A.; Nicholas, K. M. *J. Am. Chem. Soc.* **1988**, *110*, 2004. (b) Silaware, N. D.; Goldman, A. S.; Ritter, R.; Tyler, D. R. *Inorg. Chem.* **1989**, *28*, 1231. 1488.
- (10) (a) Demas, J. N.; Harris, E. W.; McBride, R. P. *J. Am. Chem. Soc.* **1977**, *99*, 3547. (b) Demas, J. N.; Harris, E. W.; Flynn, C. M.; Diemente, D. *J. Am. Chem. Soc.* **1975**, *97*, 3838. (c) Gao, R.; Ho, D. G.; Hernandez, B.; Selke, M.; Murphy, D.; Djurovich, P. I.; Thompson, M. E. *J. Am. Chem. Soc.* **2002**, *124*, 14828.
- (11) Lo, K. K. W.; Ng, D. C. M.; Chung, C. K. *Organometallics* **2001**, *20*, 4999–5001.
- (12) Nazeeruddin, Md. K.; Humphry-Baker, R.; Berner, D.; Rivier, S.; Zuppiroli, L.; Graetzel, M. *J. Am. Chem. Soc.* **2003**, *125*, 8790–8797.
- (13) Sauvage, J.-P.; Collin, J.-P.; Chambron, J.-C.; Guillerez, S.; Coudret, C.; Balzani, V.; Barigelletti, F.; De Cola, L.; Flamigni, L. *Chem. Rev.* **1994**, *94*, 993.
- (14) Barigelletti, F.; Flamigni, L.; Balzani, V.; Collin, J.-P.; Sauvage, J.-P.; Sour, A.; Constable, E. C.; Cargill-Thompson, A. M. W. *J. Am. Chem. Soc.* **1994**, *116*, 7692–7699.

- (15) Maestri, M.; Armaroli, N.; Balzani, V.; Constable, E. C.; Cargill-Thompson, A. M. W. *Inorg. Chem.* **1995**, *34*, 2759.
- (16) Collin, J.-P.; Dixon, I. M.; Sauvage, J.-P.; Williams, J. A. G.; Barigelletti, F.; Flamini, L. *J. Am. Chem. Soc.* **1999**, *121*, 5009.
- (17) In this ligand, the Br functionality has been introduced in view of further synthetic developments via metal-mediated coupling reactions.
- (18) Biscyclometalated complexes of dppy-related ligands with Pt(II) (see, e.g., Yam, V. W. W.; Tang, R. P. L.; Wong, K. M. C.; Lu, X. X.; Cheung, K. K.; Zhu, N. *Chem.—Eur. J.* **2002**, *8*, 4066) and Au(III) (see, e.g., Wong, K. H.; Cheung, K. K.; Chan, M. C. W.; Che, C. M. *Organometallics* **1998**, *17*, 3505) have been reported. A monocyclometalated dppy complex of Ir(III) has also been reported (Albeniz, A. C.; Schulte, G.; Crabtree, R. H. *Organometallics* **1992**, *11*, 242).
- (19) Cave, G. W. V.; Raston, C. L. *J. Chem. Soc., Perkin Trans. 1* **2001**, 3258.

was extracted with water and dichloromethane. The aqueous layer was discarded, and the organic layer was rotovapped to dryness. The residue was dissolved in a minimum of acetonitrile, filtered, and precipitated by addition to water. The pure product was collected by filtration and air-dried. Yield: 53 mg (38%). ^1H NMR (400 MHz, CD_3CN): δ 8.85 (s, $\text{H}_{\text{D}3',5'}$, 2H), 8.65 (dd, $J^{\text{d}} = 6.0$ Hz, $J^{\text{d}} = 4.0$ Hz, $\text{H}_{\text{P}6}$, 2H), 8.31 (s, $\text{H}_{\text{P}3',5'}$, 2H), 8.13 (d, $J^{\text{d}} = 8.0$ Hz, H_{Tb} , 2H), 8.16 (d, $J^{\text{d}} = 7.0$ Hz, H_{Db} , 2H), 8.07 (d, $J^{\text{d}} = 8.0$ Hz, $\text{H}_{\text{D}6}$, 2H), 7.98 (t, $J^{\text{c}} = 6.5$ Hz, $\text{H}_{\text{P}5'}$, 2H), 7.93 (d, $J^{\text{d}} = 8.0$ Hz, H_{Tc} , 2H), 7.86 (dd, $J^{\text{d}} = 7.0$ Hz, $J^{\text{d}} = 1.0$ Hz, $\text{H}_{\text{P}3}$, 2H), 7.54 (d, $J^{\text{d}} = 7.5$ Hz, H_{Dc} , 2H), 7.28 (ddd, $J^{\text{d}} = 7.0$ Hz, $J^{\text{d}} = 6.0$ Hz, $J^{\text{d}} = 1.0$ Hz, $\text{H}_{\text{P}4}$, 2H), 7.03 (ddd, $J^{\text{d}} = 7.0$ Hz, $J^{\text{d}} = 7.0$ Hz, $J^{\text{d}} = 0.5$ Hz, $\text{H}_{\text{D}5}$, 2H), 6.78 (ddd, $J^{\text{d}} = 7.0$ Hz, $J^{\text{d}} = 6.5$ Hz, $J^{\text{d}} = 1.0$ Hz, $\text{H}_{\text{D}4}$, 2H), 6.29 (ddd, $J^{\text{d}} = 6.0$ Hz, $J^{\text{d}} = 6.0$ Hz, $J^{\text{d}} = 0.5$ Hz, $\text{H}_{\text{D}3}$, 2H), 2.46 (s, H_{Da} , 3H). ^{13}C NMR (100 MHz, CD_3CN): δ 166.8, 165.0, 158.1, 153.9, 152.9, 151.1, 147.9, 147.7, 141.9, 141.7, 138.5, 137.9, 135.9, 135.5, 134.6, 133.6, 130.9, 130.8, 128.8, 128.3, 126.9, 126.0, 124.9, 122.8, 115.1, 21.3. MS (ESI): m/z 899.7 ($[\text{M} - \text{NO}_3]^+$ requires 900.1). X-ray diffraction quality crystals were grown by slow diffusion of diisopropyl ether into a solution in acetonitrile.

Apparatus and Procedures. The solvent for the spectroscopic measurements, acetonitrile, was of spectroscopic grade and used as received. The solutions used in the photochemical experiments were degassed with argon. Cyclic voltammetric (CV) measurements were carried out on argon-purged 1 mmol sample solutions in acetonitrile (Romil, Hi-dry), containing $[\text{TBA}]\text{PF}_6$ (0.1 mol, Fluka, electrochemical grade, 99%, oven-dried). A conventional three-electrode cell assembly was used for the CV measurements: a saturated calomel electrode (SCE; $\varnothing = 6$ mm, AMEL) and a platinum wire, both separated from the test solution by a frit, were used as reference and counter electrodes, respectively; a glassy carbon electrode (8 mm 2 , AMEL) was used as a working electrode. Cyclic voltammograms were recorded at different scan rates in the range 50 ± 500 mV s $^{-1}$ at room temperature.

UV/vis spectra were recorded with a Perkin-Elmer LAMBDA40 spectrophotometer. Emission spectra were taken on a Perkin-Elmer MPF44E or on a Spex Fluoromax-2 spectrofluorimeter, equipped with Hamamatsu R3896 tubes. The emission spectra were corrected for the instrumental response by calibration with an NBS standard quartz-halogen lamp. Emission quantum yields were measured at room temperature (20 °C) with the optically dilute method, calibrating the spectrofluorimeter with a standard lamp. $[\text{Ru}(\text{bipy})_3]^{2+}$ in deaerated acetonitrile solution was used as a quantum yield standard, assuming a value of 0.062.²⁰

^1H and ^{13}C NMR experiments were performed in CD_3CN at 400 and 100 MHz, on a JEOL EX400 spectrometer. Nanosecond flash photolysis was performed by irradiating the sample with 6 ± 8 ns (fwhm) pulses of a Continuum Surelight II Nd:Yag laser (10 Hz repetition rate) and using a pulsed Xe lamp perpendicular to the laser beam as the probing light. The desired excitation wavelength was obtained by frequency tripling (355 nm). The 150 W Xe lamp was equipped with an Applied Photophysics model 40 power supply and Applied Photophysics model 410 pulsing unit (2 ms pulses). A shutter, Oriel model 71445, placed between the lamp and the sample was opened for 100 ms to prevent photomultiplier tube (PMT) fatigue and photodecomposition. Suitable pre- and postcutoff and band-pass filters were used to prevent photodecomposition, and scattered light from the laser. The light was collected in an LDC Analytical monochromator, detected by a R928 PTM (Hamamatsu),

Table 1. Crystallographic Data for $\text{I} \cdot \text{NO}_3 \cdot 2\text{H}_2\text{O}$

empirical formula	$\text{C}_{45}\text{H}_{35}\text{BrN}_5\text{IrO}_5$	no. of measd reflns	36873
fw	997.89	no. of unique reflns	7964
space group	$P2_1/n$	R_{int}	0.077
cryst syst	monoclinic	no. of obsd reflns	6044
$a/\text{\AA}$	17.4308(4)	$[I \geq 2\sigma(I)]$	
$b/\text{\AA}$	9.0312(2)	$\theta_{\text{min}} - \theta_{\text{max}}/^\circ$	4–26
$c/\text{\AA}$	26.7601(7)	hkl ranges	–21,+21;
$\beta/^\circ$	104.496(1)		–11,+11;
$V/\text{\AA}^3$	4078.5(2)		–27,+33
Z	4	$R1(F^2)$ (obsd reflns)	0.0591
$D/\text{g cm}^{-3}$	1.625	$wR2(F^2)$ (all reflns)	0.1418
$F(000)$	1968	no. of variables	544
$\mu(\text{Mo K}\alpha)/\text{cm}^{-1}$	43.06	goodness of fit	1.114

and recorded on a Lecroy 9360 (600 MHz) oscilloscope. The laser oscillator, Q-switch, lamp, shutter, and trigger were externally controlled with a digital logic circuit, which allowed for synchronous timing. The absorption transient decays were plotted as $\Delta A = \log(I_0/I_t)$ vs time, where I_0 is the monitoring light intensity prior to the laser pulse and I_t is the observed signal at delay time t . Transient spectra were obtained from the decays measured at various wavelengths, by sampling the absorbance changes at constant delay time. Emission lifetimes in the microsecond time range were measured with the same laser/monochromator/phototube setup used for the flash photolysis experiments. Electrochemical measurements were carried out with an AMEL 552 potentiostat, an AMEL 568 programmable function generator, an AMEL 560/a interface, and an AMEL model 863 X/Y recorder. All the low-temperature experiments were measured on Oxford Instruments DN 704 cryostatic equipment with quartz windows and a standard 1 cm spectrofluorimetric cuvette.

X-ray Structure Determinations. Crystal data of the title compound were collected on a Nonius Kappa CCD diffractometer using graphite-monochromated Mo K α radiation ($\lambda = 0.7107$ Å) at room temperature (295 K). The data set was integrated with the Denzo-SMN package²¹ and corrected for Lorentz polarization and absorption (SORTAV²²) effects. The crystal parameters and other experimental details of the data collections are summarized in Table 1. The structure was solved by direct methods (SIR97)²³ and refined by full-matrix least-squares methods with all non-hydrogen atoms anisotropic and hydrogen atoms included in calculated positions, riding on their carrier atoms. All calculations were performed using SHELXL-97²⁴ and PARST²⁵ implemented in the WINGX system of programs.²⁶

The structure displays some disorder within the Br-phenyl ring, where four atoms were refined over two distinct positions, the nitro anion, where two oxygen atoms were refined over two positions, and the oxygen of a water molecule, which was refined isotropically. The hydrogen atoms of both water molecules were not localized.

Computational Details. Calculations on the electronic ground state of the complex were carried out using B3LYP density functional theory.²⁷ “Double- ζ ”-quality basis sets were employed

(20) Calvert, J. M.; Caspar, J. V.; Binstead, R. A.; Westmoreland, T. D.; Meyer, T. J. *J. Am. Chem. Soc.* **1982**, *104*, 6620.

- (21) Otwinowski, Z.; Minor, W. In *Methods in Enzymology*; Carter, C. W., Sweet, R. M., Eds.; Academic Press: London, 1997; Vol. 276, Part A, p 307.
- (22) Blessing, R. H. *Acta Crystallogr.* **1995**, *A51*, 33.
- (23) Altomare, A.; Burla, M. C.; Camalli, M.; Cascarano, G. L.; Giacovazzo, C.; Guagliardi, A.; Moliterni, A. G. G.; Polidori, G.; Spagna, R. *J. Appl. Crystallogr.* **1999**, *32*, 115.
- (24) Sheldrick, G. M. *SHELXL97, Program for Crystal Structure Refinement*; University of Göttingen, Göttingen, Germany, 1997.
- (25) Nardelli, M. *J. Appl. Crystallogr.* **1995**, *28*, 659.
- (26) Farrugia, L. J. *J. Appl. Crystallogr.* **1999**, *32*, 837.
- (27) (a) Lee, C.; Yang, W.; Parr, R. G. *Phys. Rev. B* **1988**, *37*, 785. (b) Becke, A. D. *J. Chem. Phys.* **1993**, *98*, 5648. (c) P. Jeffrey Hay. *J. Phys. Chem. A* **2002**, *106*, 1634–1641.

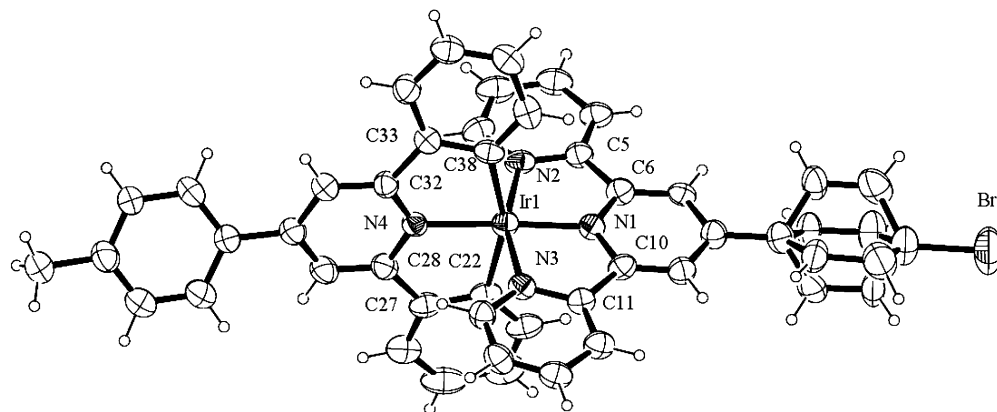


Figure 1. ORTEP³⁰ view of the complex cation of the title compound displaying the thermal ellipsoids at 30% probability. Both the orientations of the disordered Br-phenyl ring are shown.

for the ligands (6-31G) and the Ir (LANL2DZ). A relativistic effective core potential (ECP) on Ir²⁸ replaced the inner core electrons, leaving the outer core [(5s)2(5p)6] electrons and the (5d)6 valence electrons of Ir(III). The geometries were fully optimized without symmetry constraints. At the respective ground-state geometries, time-dependent density functional theory (TDDFT) calculations using the B3LYP functional were performed. All calculations were performed using the Gaussian 98 package.²⁹

Results and Discussion

Synthesis. The synthesis of this new complex was achieved in ethylene glycol at 200 °C for 1 h. The reaction required vigorous degassing with argon and silver to remove the chloride ions. Exposure to low levels of light did not seem to affect the yield of the reaction. These reaction conditions are harsh, even for iridium complexes, which are notorious for requiring high temperatures to overcome the inertness of the coordination sphere. In the case of iridium–bisterpyridine complexes, temperatures are required to be high (140–180 °C), and yet strictly controlled to stop the formation of cyclometalated complexes. Light must also be strictly excluded for the same reason. Here, no reaction can be seen at less than 180 °C, and the product is formed in the same conditions found to favor cyclometalated products in bisterpyridine reactions. Lengthening the reaction time seemed only to increase the amount of a black, insoluble byproduct. The yield of the reaction was invariably low (34%); however, the desired product was the only product isolable. A small amount of a yellow, highly fluorescent compound was easily removed using chromatography on silica gel.

(28) Hay, P. J.; Wadt, W. R. *J. Chem. Phys.* **1985**, *82*, 299–310.

(29) Frisch, M. J.; Trucks, G. W.; Schlegel, H. B.; Scuseria, G. E.; Robb, M. A.; Cheeseman, J. R.; Zakrzewski, V. G.; Montgomery, J. A.; Stratmann, R. E.; Burant, J. C.; Dapprich, S.; Millam, J. M.; Daniels, A. D.; Kudin, K. N.; Strain, M. C.; Farkas, O.; Tomasi, J.; Barone, V.; Cossi, M.; Cammi, R.; Mennucci, B.; Pomelli, C.; Adamo, C.; Clifford, S.; Ochterski, J.; Petersson, G. A.; Ayala, P. Y.; Cui, Q.; Morokuma, K.; Malick, D. K.; Rabuck, A. D.; Raghavachari, K.; Foresman, J. B.; Cioslowski, J.; Ortiz, J. V.; Stefanov, B. B.; Liu, G.; Liashenko, A.; Piskorz, P.; Komaromi, I.; Gomperts, R.; Martin, R. L.; Fox, D. J.; Keith, T.; Al-Laham, M. A.; Peng, C. Y.; Nanayakkara, A.; Gonzalez, C.; Challacombe, M.; Gill, P. M. W.; Johnson, B. G.; Chen, W.; Wong, M. W.; Andres, J. L.; Head-Gordon, M.; Replogle, E. S.; Pople, J. A. *Gaussian 98*, revision A.11; Gaussian, Inc.: Pittsburgh, PA, 1998.

Table 2. Selected Bond Distances (Å) and Angles (deg)

Distances			
Ir1–N1	1.943(6)	Ir1–N4	2.022(6)
Ir1–N2	2.044(6)	Ir1–C22	2.122(9)
Ir1–N3	2.053(6)	Ir1–C38	2.094(9)
Angles			
N1–Ir1–N2	79.6(3)	N4–Ir1–C22	79.6(3)
N1–Ir1–N3	80.3(2)	N4–Ir1–C38	78.9(3)
N1–Ir1–N4	177.6(3)	C22–Ir1–C38	158.3(3)
N1–Ir1–C22	98.2(3)	Ir1–N1–C6	119.3(5)
N1–Ir1–C38	103.4(3)	Ir1–N1–C10	118.8(5)
N2–Ir1–N3	159.9(3)	Ir1–N2–C5	113.8(5)
N2–Ir1–N4	101.4(2)	Ir1–N3–C11	113.4(5)
N2–Ir1–C22	93.5(3)	Ir1–N4–C28	118.5(4)
N1–Ir1–C38	88.1(3)	Ir1–N4–C32	119.8(5)
N3–Ir1–N4	98.7(2)	Ir1–C22–C27	111.8(6)
N3–Ir1–C22	89.4(3)	Ir1–C38–C33	112.5(6)
N3–Ir1–C38	96.4(3)		

Crystal Structure. An ORTEP³⁰ view is shown in Figure 1. Selected bond distances and angles are given in Table 2. The iridium(III) center is in a distorted octahedral geometry owing to the constraints of the terpyridine and cyclometalated ligand. The distortions of the coordinated terpyridine ligand are associated with significant narrowing of N (peripheral)–Ir–N (middle) angles of 79.6(3)° and 80.3(2)° and with a shortening of Ir–N1 (middle) distances to 1.943(6) Å with respect to the Ir–N2 and Ir–N3 bonds of 2.044(6) and 2.053(6) Å, respectively. These data are in perfect agreement with the other structures of Ir(III)–terpyridine derivatives,^{16,31,32} where Ir–N (middle) distances range from 1.92 to 1.98 Å, while Ir–N (peripheral) distances range from 2.03 to 2.07 Å. The three pyridine rings P1, P2, and P3 (which contain the N1, N2, and N3 nitrogens, respectively) lie on the same plane, making the following dihedral angles: P1–P2 = 2.2(2)°, P1–P3 = 1.9(2)°, and P2–P3 = 4.1(2)°.

The cyclometalated ligand is in an approximately perpendicular arrangement with respect to the terpyridine ligand with a dihedral angle between the pyridine rings P1 and P4 (which contains the N4 nitrogen) of 85.4(3)°. The Ir–C

(30) Burnett, M. N.; Johnson, C. K. *ORTEP-III: Oak Ridge Thermal Ellipsoids Plot Program for Crystal Structure Illustrations*; Oak Ridge National Laboratory Report ORNL-6895; Oak Ridge National Laboratory: Oak Ridge, TN, 1996.

(31) Vogler, L. M.; Scott, B.; Brewer, K. J. *Inorg. Chem.* **1993**, *32*, 898.

(32) Lo, K. K.-W.; Chung, C.-K.; Ng, D. C.-M.; Zhu, N. *New J. Chem.* **2002**, *26*, 81.

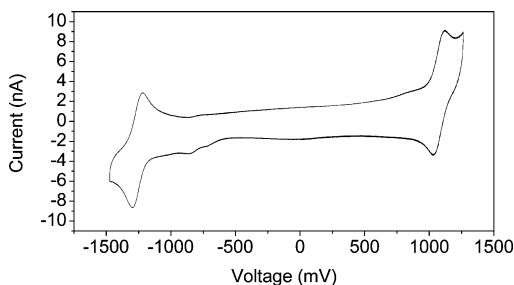


Figure 2. Cyclic voltammogram of **1** (scan rate 100 mV/s) recorded in degassed acetonitrile with 0.1 M TBAPF₆ as electrolyte (SCE reference electrode).

distances of 2.122(9) and 2.094(9) Å, for Ir–C22 and Ir–C38 bonds, respectively, and the Ir–N4 distance of 2.022(6) Å seem to be in some disagreement with those observed in other Ir(III) cyclometalated complexes^{5,33–37} where, in general, Ir–C bond distances are shorter than Ir–N bond distances. The discrepancies can be elucidated by an accurate analysis of bond lengths. In many Ir(III) complexes a cyclometalated carbon *trans* to a pyridine nitrogen gives rise to an elongation of the Ir–N bond up to a length of 2.24 Å. The Ir–C bonds on the other hand remain in the somewhat short range of 1.99–2.03 Å. There are a few cases where the nitrogen atoms are in *trans* positions to each other and the distances shorten to 2.01–2.06 Å, while carbon atoms which are *trans* to each other give rise to longer Ir–C distances in the range 2.05–2.08 Å. From all these data it is evident that the carbon atom exerts a significant *trans* effect on both Ir–N (pyridine) and Ir–C (phenyl) distances. Accordingly, the lengthening of Ir–C bonds in the present structure can be justified by a strong mutual *trans* effect between C22 and C38, while Ir–N4 remains short, being in a *trans* position with respect to another pyridine nitrogen. The cyclometalated ligand displays a slight distortion from planarity; the pyridine P4 and the phenyls P5 (C22–C27 ring) and P6 (C33–C38 ring) make the following dihedral angles: P4–P5 = 4.4(2)°, P4–P6 = 10.0(2)°, and P5–P6 = 12.8(3)°.

Electrochemistry. The complex exhibits two reversible electrochemical processes. The cyclic voltammogram is shown in Figure 2. At negative potentials there is a single one-electron process at –1.27 V vs SCE. We assign this process to the reduction of the terpyridine ligand. This assignment is supported by DFT calculations that show that the lowest unoccupied molecular orbital (LUMO) is mainly localized on the terpyridine ligand (vide infra).³⁸ This potential is more negative than that of the bis(tolylterpyridine) analogue,¹⁶ which has a reduction at –0.81 V. This is due

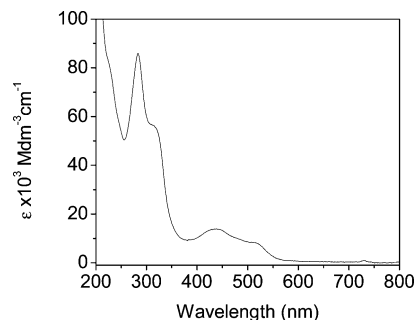


Figure 3. Electronic absorption spectrum of the complex in an acetonitrile solution.

to the stabilizing effect of the nearby 3+ charge on the iridium in the latter compared to a formal 1+ charge in the former.

There is also a reversible one-electron oxidation at +1.08 V. This potential cannot be simply assigned to metal oxidation, due to the strong covalency of the Ir–C bonds. In fact, DFT calculations show that the highest occupied molecular orbitals (HOMOs) of **1** are substantially delocalized over the Ir–dppy fragment (vide infra).³⁸ This potential is not far from those found for other Ir(III) cyclometalated complexes with two coordinated carbons and four nitrogen atoms.^{39,40} Cyclometalated complexes in which there is only one carbon attached to the iridium center have very high oxidation potentials (typically >2 V),^{16,40} whereas those with three cyclometalated carbons have oxidation potentials in the region of 0.7 V.⁵ This underlines the general effect of the number of cyclometalated carbons on the oxidation potential of these complexes. It can be noticed that, among the Ir(III) cyclometalated complexes with two coordinated carbons and four nitrogen atoms, our complex is somewhat easier to oxidize than previously reported cases (e.g., +1.40 V⁴⁰ and +1.23 V³⁹). It should be remarked, however, that the coordination sphere with two *trans* carbons is unique to this complex. A similar effect of the *cis* vs *trans* carbon arrangement has been observed for the triscyclometalated Ir(ppy)₃,⁵ where the common *fac* isomer is easier to oxidize by ca. 0.1 V than the less common *mer* isomer. The effect is larger in the present case, however, because of the more rigid coordination geometry, with the two negatively charged destabilizing *trans* carbons belonging to the same terdentate ligand.

Electronic Absorption Spectrum. The electronic absorption spectrum of the complex is shown in Figure 3. There are two strong absorptions in the UV region at 284 nm ($\epsilon = 97500$) and 320 nm ($\epsilon = 66000$), which can be assigned as LC π – π^* transitions. Less usually for iridium complexes, a well-resolved band system is observed in the visible region with two strong bands at 520 nm ($\epsilon = 19100$) and 437 nm ($\epsilon = 25500$) and a shoulder at 484 nm ($\epsilon = 21200$). It is tempting to assign these bands as MLCT in nature. However, care must be taken in the case of iridium cyclometalated

(33) Garces, F. O.; Dedeian, K.; Keder, N. L.; Watts, R. I. *Acta Crystallogr.* **1993**, C49, 1117.

(34) Colombo, M. G.; Brunold, T. C.; Riedener, T.; Güdel, H. U.; Förtsch, M.; Bürgi, H.-B. *Inorg. Chem.* **1994**, 33, 545.

(35) Neve, F.; Crispini, A.; Campagna, S.; Serroni, S. *Inorg. Chem.* **1999**, 38, 2250.

(36) Lamansky, S.; Djurovich, P.; Murphy, D.; Abdel-Razzaq, F.; Kwong, R.; Tsyba, I.; Bortz, M.; Mui, B.; Bau, R.; Thompson, M. E. *Inorg. Chem.* **2001**, 40, 1704.

(37) Grushin, V. V.; Herron, N.; LeCloux, D. D.; Marshall, W. J.; Petrov, V. A.; Wang, Y. *Chem. Commun.* **2001**, 1494.

(38) A full account of such calculations will be given in a subsequent paper (M. Polson and M. Ravaglia, manuscript in preparation).

(39) Ohsawa, Y.; Sprouse, S.; King, K. A.; DeArmond, M. K.; Hanck, K. W.; Watts, R. J. *J. Phys. Chem.* **1987**, 91, 1047.

(40) Mamo, A.; Stefio, I.; Parisi, M. F.; Credi, A.; Venturi, M.; Di Pietro, C.; Campagna, S. *Inorg. Chem.* **1997**, 36, 5947.

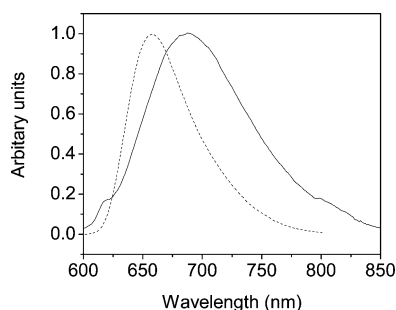


Figure 4. Room-temperature (solid line) and 77 K (dashed line) emission spectra of the title complex. Both spectra were recorded in acetonitrile, with the room-temperature sample having been degassed with argon.

complexes in the use of localized descriptions of molecular orbitals and transitions, as the HOMO orbitals may be significantly delocalized over the cyclometalating phenyls.⁵ In fact, for several of such systems mixed descriptions seem to be more appropriate. For instance, in Ir(ppy)₃ the lowest excited state is considered to have mixed-ligand-centered MLCT (LC-MLCT) character.^{5,7,36} In the case of **1**, DFT calculations indicate that the visible transitions occur from orbitals localized on the Ir–dppy fragment to orbitals localized on the terpyridine ligand.³⁸ Therefore, besides Ir → tpy MLCT, an appreciable amount of dppy → tpy ligand-to-ligand charge transfer (LLCT) is likely to be involved in these transitions. Thus, the visible bands of **1** can be appropriately assigned as mixed MLCT–LLCT transitions.

Emission Measurements. The room-temperature emission spectrum of the complex is shown in Figure 4. The emission energy (λ_{max} , 690 nm) is much lower than for the corresponding bisterpyridine complexes (λ_{max} , 506 nm for the bis-(tolylterpyridine) analogue).¹⁶ This is due to a destabilizing effect of the two cyclometalated carbons on the donor orbitals, as already noticed in the discussion of the electrochemical data. The emission energy is also substantially lower than that of the biscyclometalated complex [Ir(ppy)₂-bipy]⁺, which emits at 606 nm. This is due to the lower energy of the terpyridine acceptor orbital (as seen in the electrochemistry) compared to the bipyridine acceptor orbital.

The nature of the emitting state can be sketched considering the aforementioned TD-DFT computational results.³⁷ At the ground-state geometry, one can analyze the calculated first excited state and correlate it to the emitting state. The calculations show that the first excited state is a triplet state whose emission wavelength (680 nm) is in excellent agreement with the experimental value (690 nm). The nature of the state follows directly from the nature of the vertical transitions involved, in this case a combination of two one-electron excitations from a pair of quasi-degenerate occupied MOs (HOMO and HOMO – 1) to the LUMO. As shown in Figure 5, the two occupied MOs are essentially localized on the Ir–dppy fragment, and the LUMO is occupied on the Ir–tpy fragment. The main charge displacement, therefore, takes place from the dppy-like to the tpy-like ligand. In simple terms, the best description of the emitting state is that of a dppy → tpy LLCT state.

The quantum yield of the emission of **1** ($\phi = 0.032$) is lower than those of common biscyclometalated iridium complexes (e.g., $\phi = 0.34$ for Ir(ppy)₂(acac)).⁷ This low quantum yield is not related to the emission lifetime. In fact, the lifetime of **1** (1.7 μs in degassed acetonitrile at room temperature) is comparable to, or longer than, those of the stronger emitters (e.g., 1.7 μs for Ir(ppy)₂(acac)⁷). This implies that the emitting state of **1** has a low radiative rate constant ($k_r = 1.9 \times 10^4 \text{ s}^{-1}$ vs, e.g., $2.1 \times 10^5 \text{ s}^{-1}$ for Ir(ppy)₂(acac)⁷). This low value may tentatively be attributed to the peculiar orbital origin of the excited state of **1** that, in contrast with common cases, adds substantial ligand-to-ligand character to the MLCT nature. The emission of the complex is strongly quenched by oxygen ($\tau = 200 \text{ ns}$ in air-saturated acetonitrile).

The emission spectrum of the complex at 77 K is also shown in Figure 4. As in the room-temperature spectrum, the emission is broad and structureless. This rules out an LC nature of the emission (which would induce prominent vibrational structure)¹⁶ and is consistent with a charge-transfer nature of the excited state. It has already been noticed that cyclometalated complexes with *trans* Ir–C bonds (such as, e.g., *mer*-Ir(ppy)₃) tend to give structureless emissions, probably because of the large excited-state distortion brought about by this geometric arrangement.⁴¹ The blue shift of the low-temperature spectrum is qualitatively consistent with a charge-transfer assignment, although its magnitude (610 cm^{-1}) is relatively small compared with those of typical MLCT transitions (e.g., 2300 cm^{-1} for [bipyIr(ppy)₂]⁺),⁴² a feature likely related to the peculiar LLCT character of the transition in **1**.

Transient Absorption Measurements. The transient electronic absorption spectrum of the complex, collected in degassed acetonitrile solution at room temperature, is shown in Figure 6. The data points were measured approximately 50 ns after the laser pulse. The decay matches well the emission decay, indicating that the transient spectrum is associated with the emissive state. Three features are clearly visible. First, there is a strong absorption in the UV region with a maximum at less than 360 nm. There is also a strong absorption in the red region with a maximum at 610 nm. Finally, there is bleaching in the visible region of a series of bands at 440, 488, and 521 nm. The bleaching features correspond very closely to the ground-state absorptions in the visible region (see Figure 3). The two absorption features are characteristic of the formation of the radical anion of a phenyl-substituted terpyridine ligand,⁴³ providing direct spectroscopic evidence for the terpyridine-localized nature of the LUMO.

(41) In Ir(ppy)₃ and similar complexes, such a distortion may lead to dissociation of the Ir–C bonds, with consequent short excited-state lifetimes and efficient *mer* → *fac* photoisomerization. It should be noticed that no deligating pathway is available in the present case, due to the tridentate nature of the biscyclometalating ligand. This is witnessed by the long excited-state lifetime.

(42) Garces, F. O.; King, K. A.; Watts, R. J. *Inorg. Chem.* **1988**, *27*, 3464.

(43) Collin, J.-P.; Guillerez, S.; Sauvage, J.-P.; Barigelletti, F.; De Cola, L.; Flamigni, L.; Balzani, V. *Inorg. Chem.* **1991**, *30*, 4230.

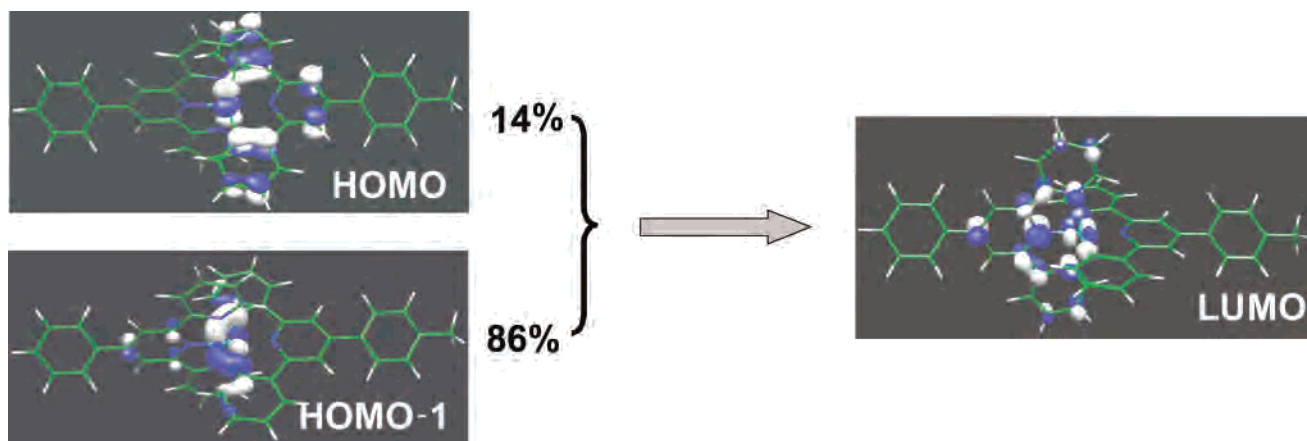


Figure 5. Molecular orbitals involved in the formation of the lowest triplet state of **1**. The excited state is represented by a combination (mixing coefficients in parentheses) of two one-electron transitions originating in a pair of quasi-degenerate HOMOs.

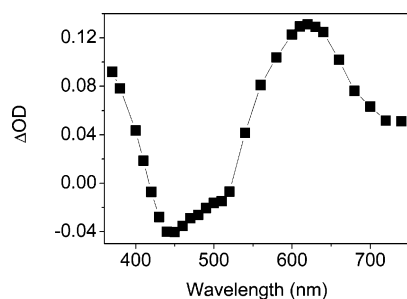
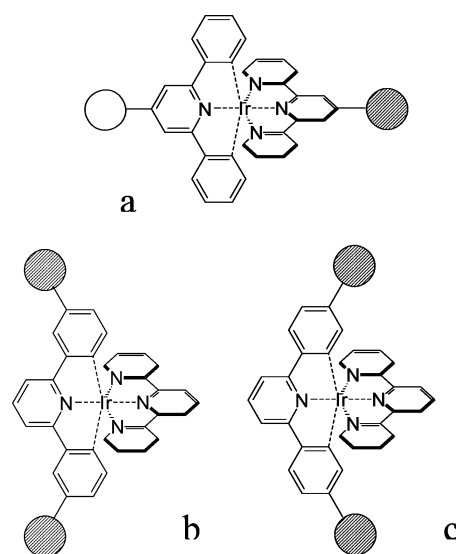


Figure 6. Transient electronic absorption spectrum of the title complex. The spectrum was recorded in degassed acetonitrile solution approximately 50 ns after the laser pulse ($\lambda_{\text{ex}} = 355$ nm).

Conclusions

This complex represents an interesting new motif in the coordination chemistry of iridium. It is the first example of an iridium bis-cyclometalated complex with dppy-type ligands. In common with bisterpyridine complexes, **1** has axial symmetry, a feature that makes it an attractive building block for the construction of extended one-dimensional supramolecular species. Compared with bisterpyridine analogues, the double cyclometalation moves the oxidation potential into an accessible electrochemical region and brings about visible absorption and long-lived emission of charge-transfer nature. The inherent asymmetry ($C \wedge N \wedge C$ and $N \wedge N \wedge N$) of the terdentate ligand set, on the other hand, brings two interesting consequences: (i) asymmetric functionalization at the two ends of the molecular axis is easy (Chart 1a); (ii) the emitting, long-lived excited state has a vectorial character, with LLCT in the dppy \rightarrow tpy direction along the molecular axis. Ongoing work on this and related systems includes a systematic study of the effects of axial substitution, as well as the application of ultrafast time-resolved techniques and computational methods to the characterization of ground and excited states. Interesting synthetic developments can also be envisioned upon functionalization at the phenyl moieties

Chart 1



of the dppy ligand (Chart 1b,c), given the abundance of available substituted aryl precursors.⁴⁴

Acknowledgment. We thank Anna Prodi and Maria Teresa Indelli for help with the electrochemical and low-temperature emission measurements. We also thank Marco Garavelli for the computational resources. Funding by the EC (Grant G5RD-CT-2002-00776, MWFM) and MIUR (Grant FIRB-RBNE019H9K) is gratefully acknowledged.

Supporting Information Available: X-ray crystallographic file in CIF format and ^1H and ^{13}C NMR spectra and structure showing the numbering scheme used to assign protons (PDF). This material is available free of charge via the Internet at <http://pubs.acs.org>.

IC0351848

(44) We thank one of the reviewers for calling our attention to this aspect.